Magnetotactic bacteria

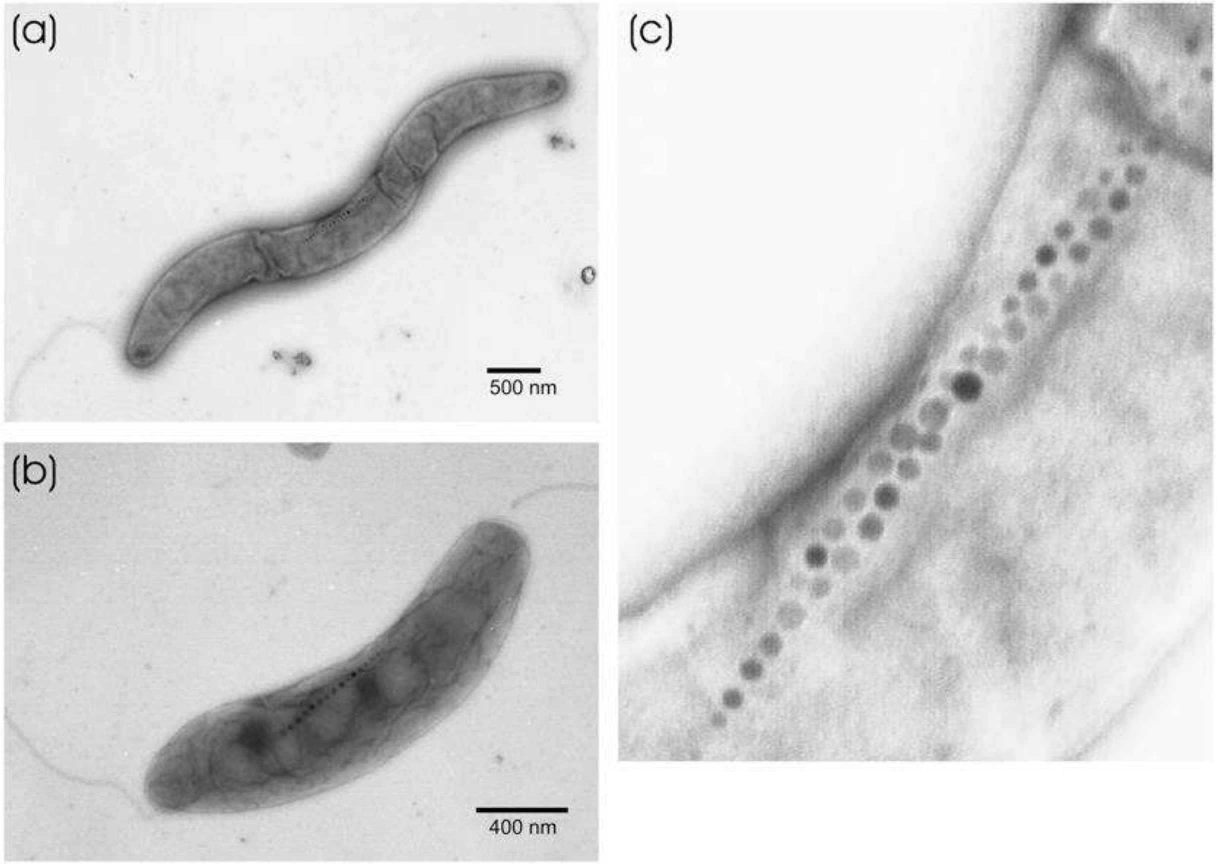

Fig.1

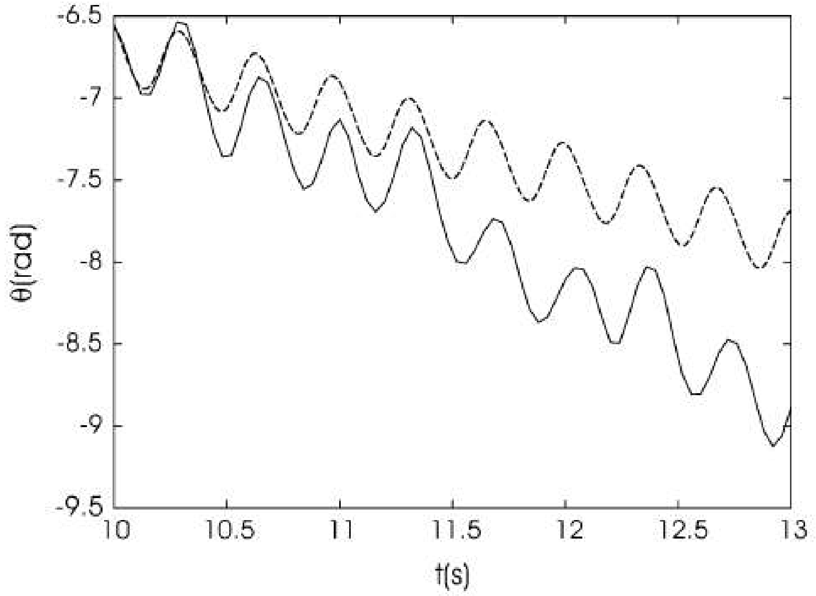

FIGURE 5 Orientation angle of a long axis of a bacterium during its back-and-forth motion. The value θ is the angle between the long axis of the bacterium and the horizontal axis of the image. The magnetic field rotates clockwise. Theoretical dependence of θ at $\omega_c/\omega = 0.205$ is shown by the dashed line. $H = 14$ Oe; $\nu = 3$ Hz.

Fig.2

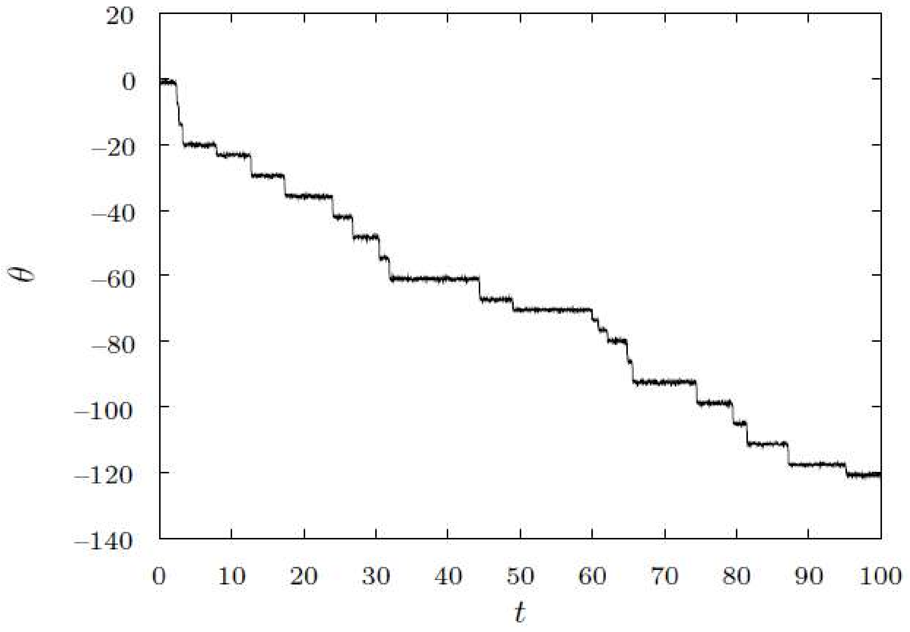

Fig. 6. Stochastic dynamics of a dipole at $\omega/\omega_c = 49/50$ and $\xi = 50$.

Fig.3

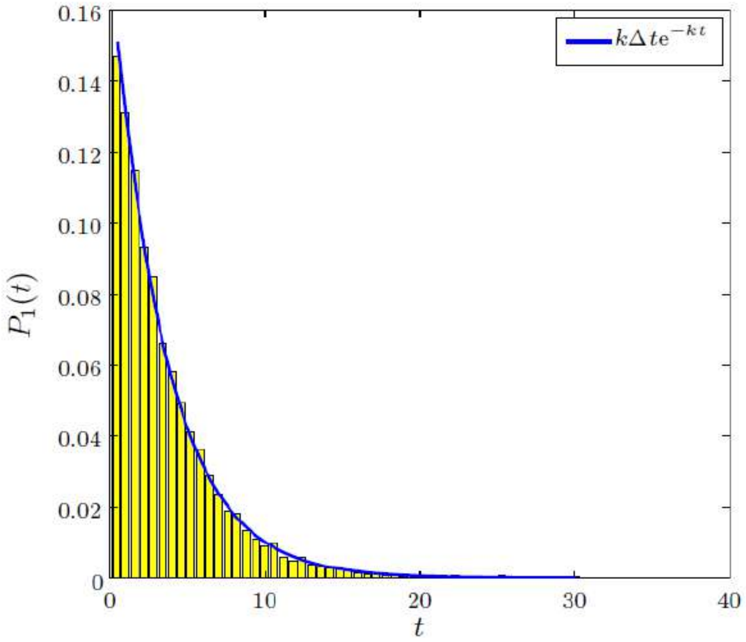

Fig. 7. Data histogram of the overturns for $\omega/\omega_c = 49/50$ and $\xi = 50$. The solid line represents the Poisson distribution function.

Fig.4

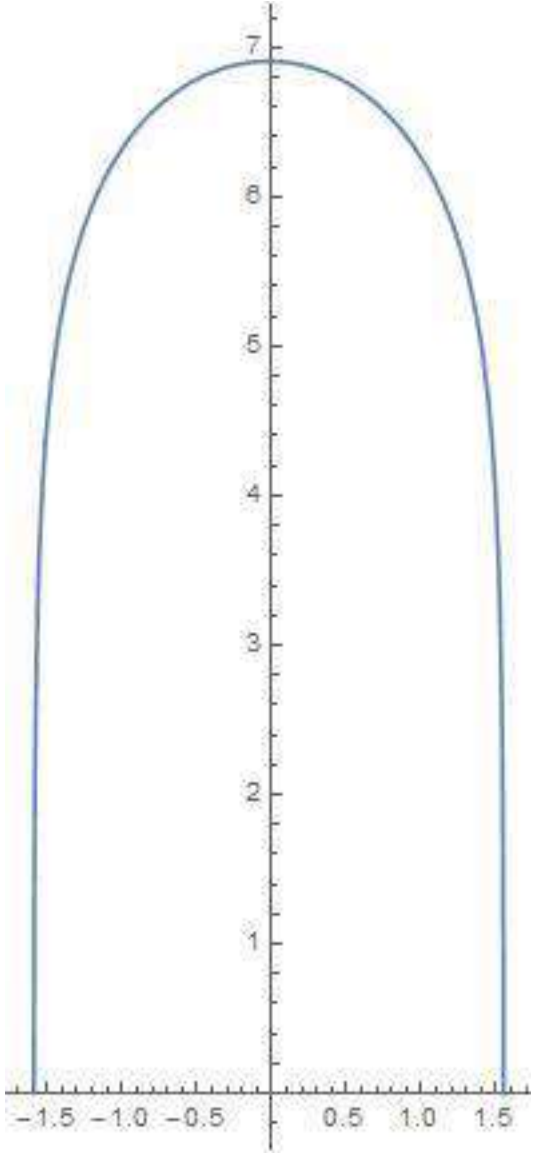

Fig.5

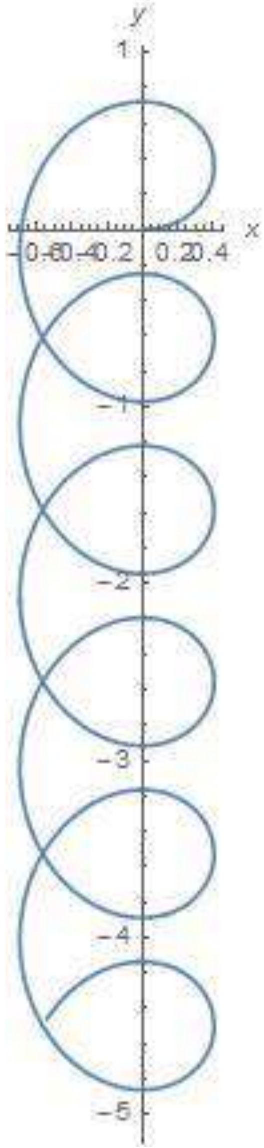

Fig.6

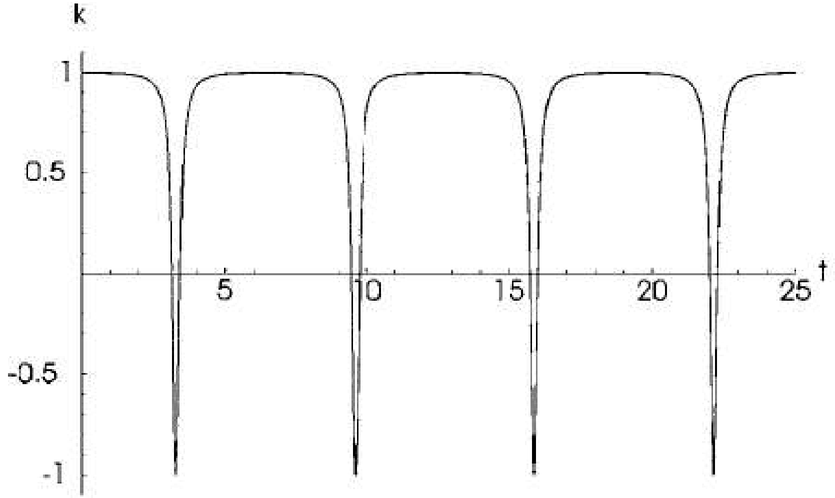

FIG. 1. Curvature of trajectory in dependence on time. γ=0.99.

Fig.7

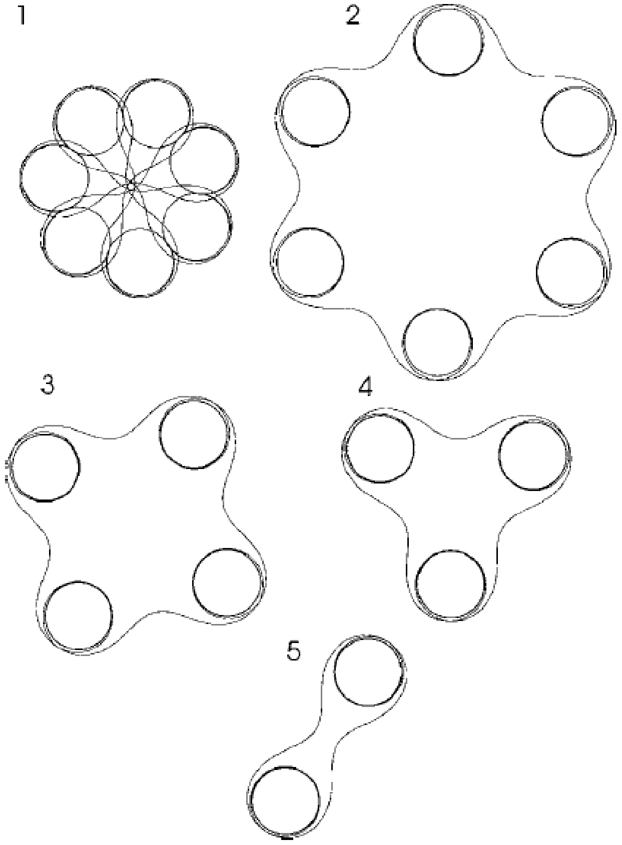

FIG. 3. Trajectories of the particle for $\sqrt{1-\gamma^2}$=7/25 (1); 6/25 (2); 4/25 (3); 3/25 (4); 2/25 (5).

Fig.8

2

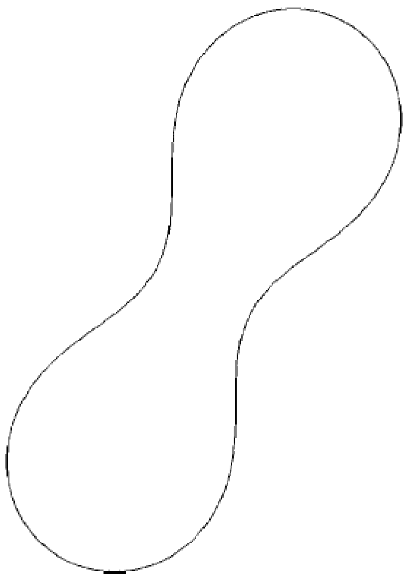

Fig.9

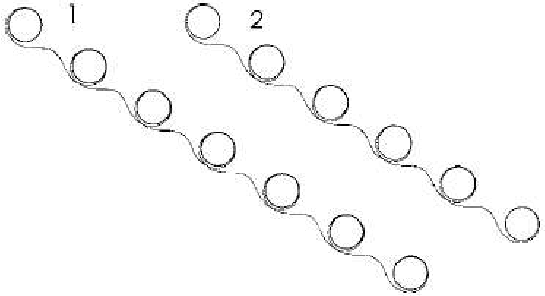

FIG. 4. Trajectories of the particle for $\sqrt{1-\gamma^2}$=5/25 (1); 1/25 (2).

Fig.10

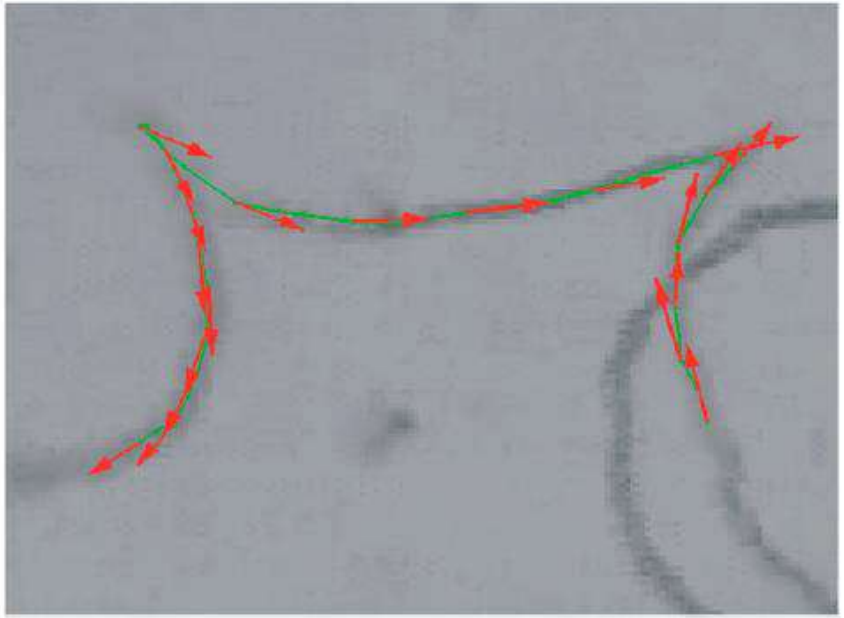

FIGURE 9 Reversals in a rotating magnetic field. $H = 10\,Oe$ and $\nu = 0.45$ Hz. The field rotates clockwise. Two reversal events can be seen. Although the long axis of the bacterium continues to rotate clockwise at the both vertices of the trajectory, due to the reversal of the motion of the bacterium, the trajectory has cusps. An increase in the curvature radius of the trajectory after reversal can also be noticed.

Fig.11

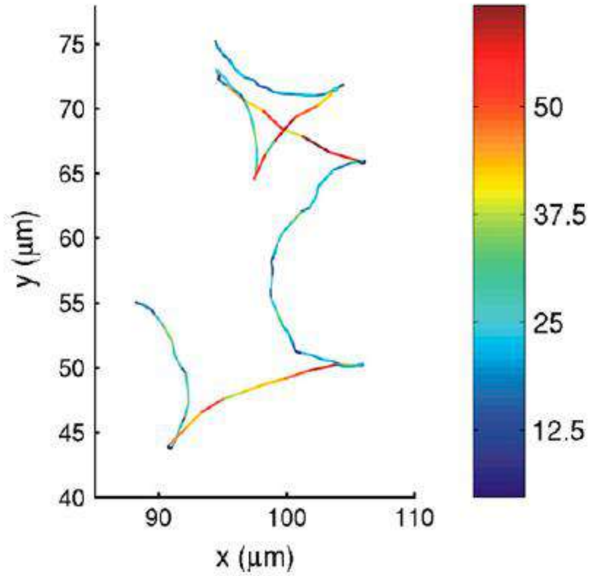

FIGURE 10 Bacterial velocity distribution at reversals. Consecutive changes from lower to higher and higher to lower speeds can be noticed at reversal events. $H = 10\,Oe$ and $\nu = 0.4$ Hz. The trajectories shown at the left are color-coded for speed as quantified by the calibration scale at the right. Numbers correspond to the values of velocity in μm/s.

Fig.12

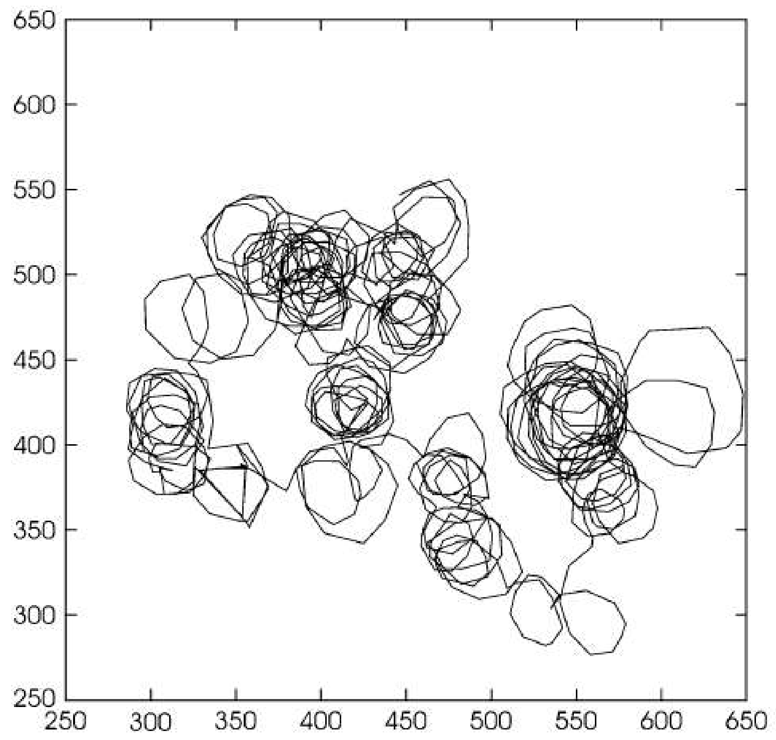

FIGURE 11 Wandering of the centers of circular trajectories due to reversals in a rotating magnetic field. $H = 10\ Oe$, and frequency slowly increases from 0.47 Hz to 0.62 Hz during 200-s-long time interval. Coordinates of bacterium are shown in pixels. 18 pixels = 3.2 μm.

Fig.13

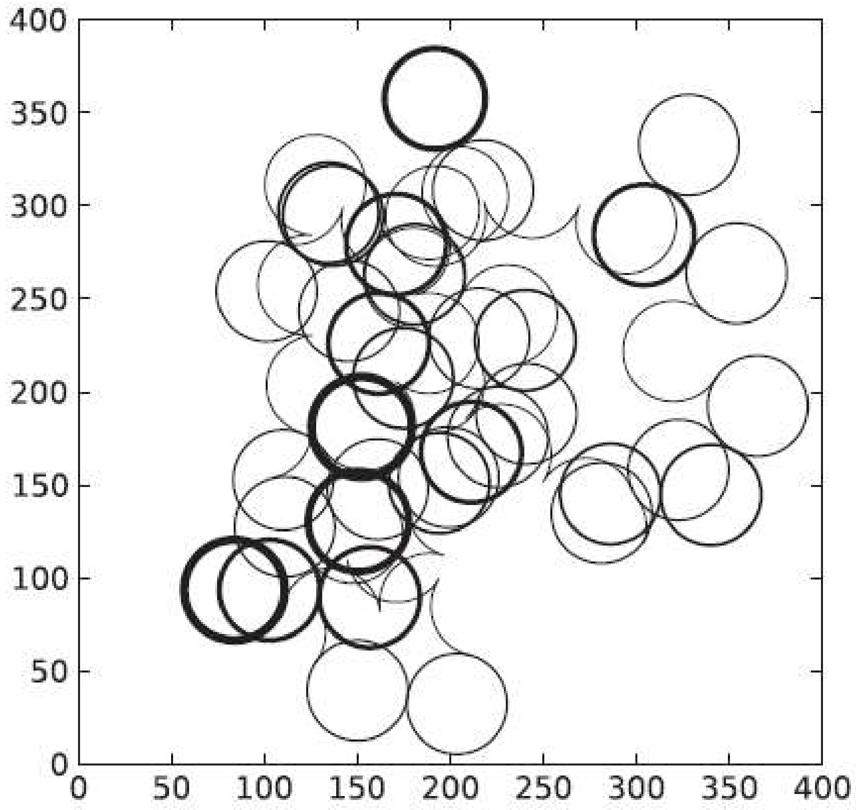

Fig. 1. Generated random trajectory of the bacterium. Line thickness is proportional to the number of full turns before switching of the swimming direction. Coordinates are shown in pixels. 18 pixels = 3.2 μm. See [6, Fig. 11] for a qualitative and quantitative comparison.

Fig.14

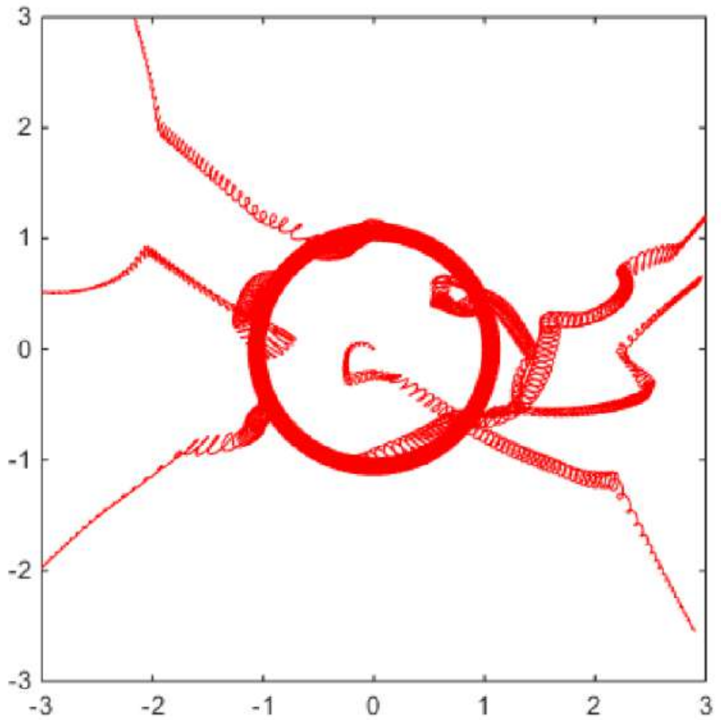

FIG. 1. Establishment of regular hexagon shown by trajectories of trajectories centers $\vec{R}_i$. Initial random positions in square $[-5, 5; -5, 5]$. $N = 7$. $\lambda = -0.1$.

Fig.15

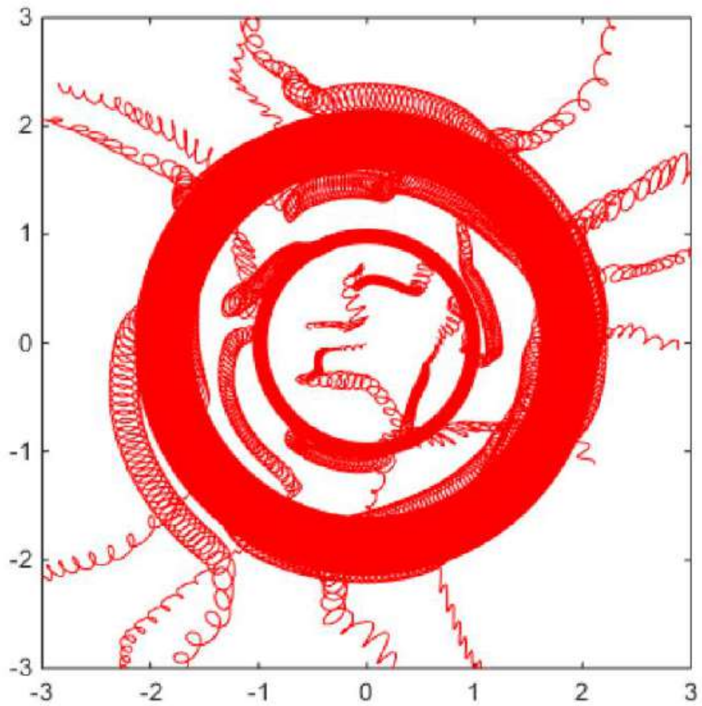

FIG. 2. Establishment of regular hexagon shown by trajectories of trajectories centers $\vec{R}_i$. Initial random positions in square $[-5, 5; -5, 5]$. $N = 19$. $\lambda = -0.1$.

Fig.16

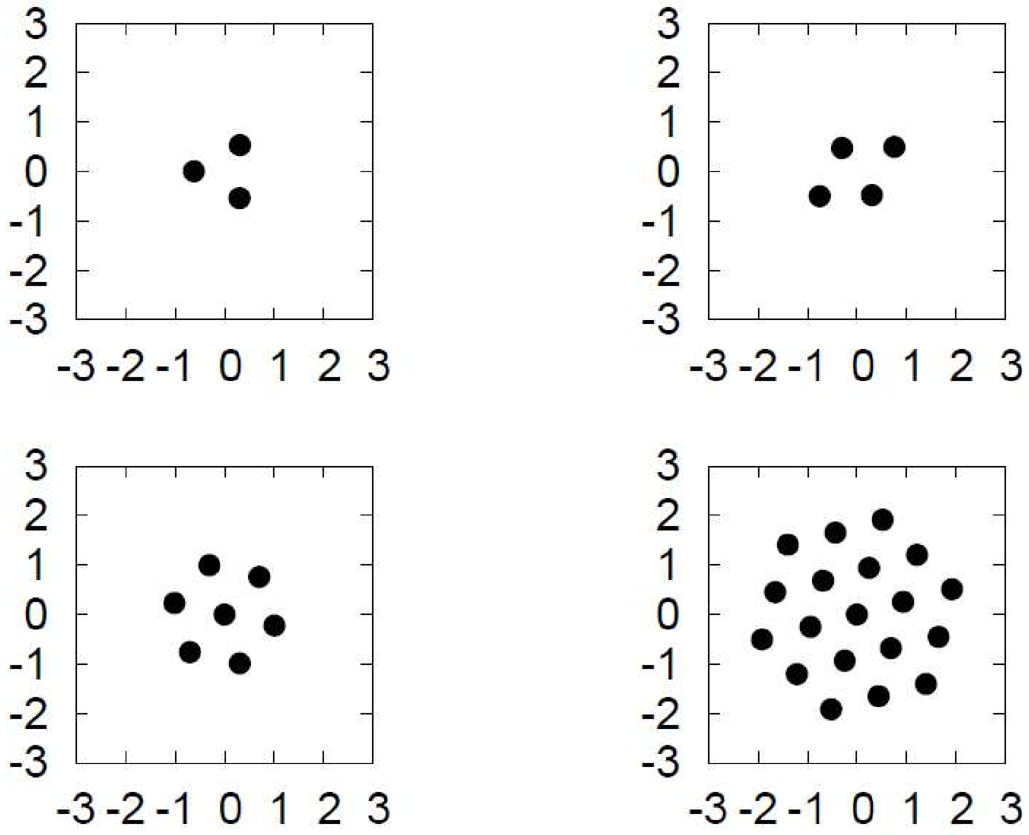

FIG. 1. Stationary rotating structures at $N = 3, 4, 7, 19. \lambda = -0.1$. Positions of particles are averaged for 10 periods of a rotating field.

Fig.17

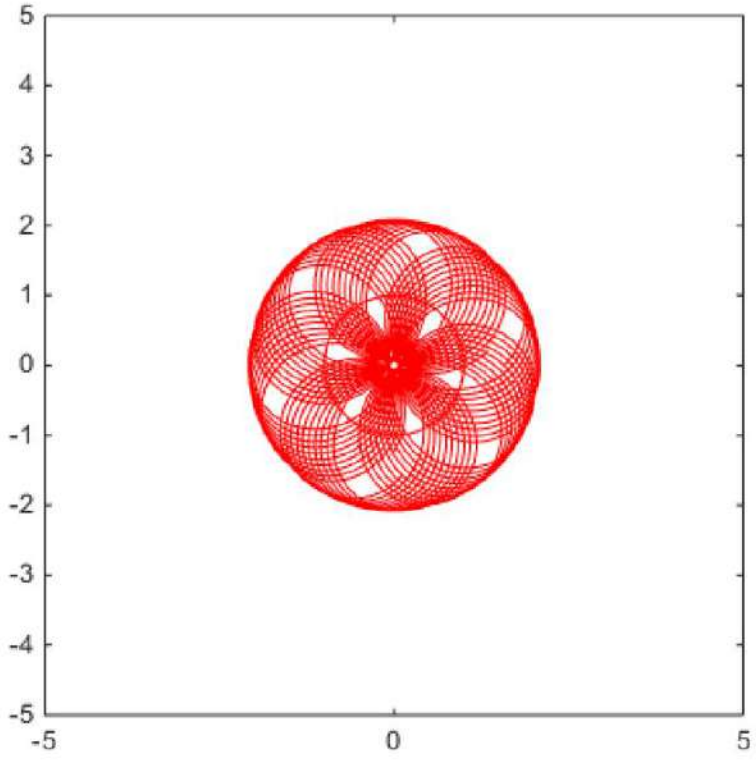

FIG. 3. Trajectories of bacteria at established mean positions of trajectory centers on the vertices of regular hexagonal structure (see Fig. 1). Initial random positions in square $[-5, 5; -5, 5]$. $N = 7$. $\lambda = -0.1$.

Fig.18

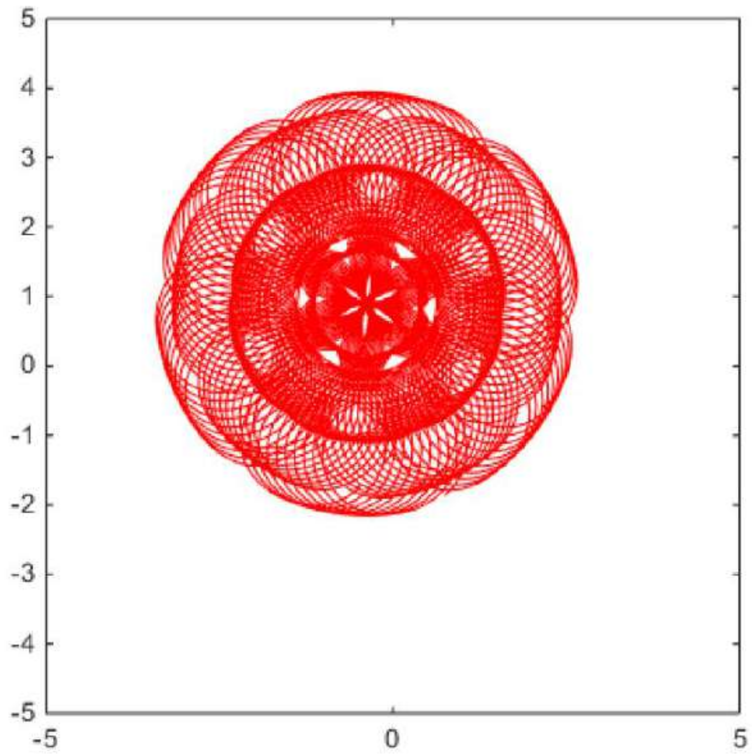

FIG. 4. Trajectories of bacteria at established mean positions of trajectory centers on the vertices of regular hexagonal structure (see Fig. 1). Initial random positions in square $[-5, 5; -5, 5]$. $N = 19$. $\lambda = -0.1$.

Fig.19

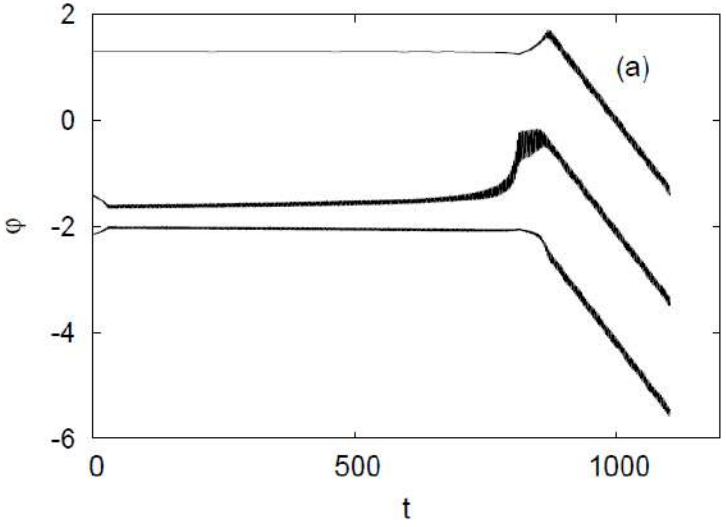

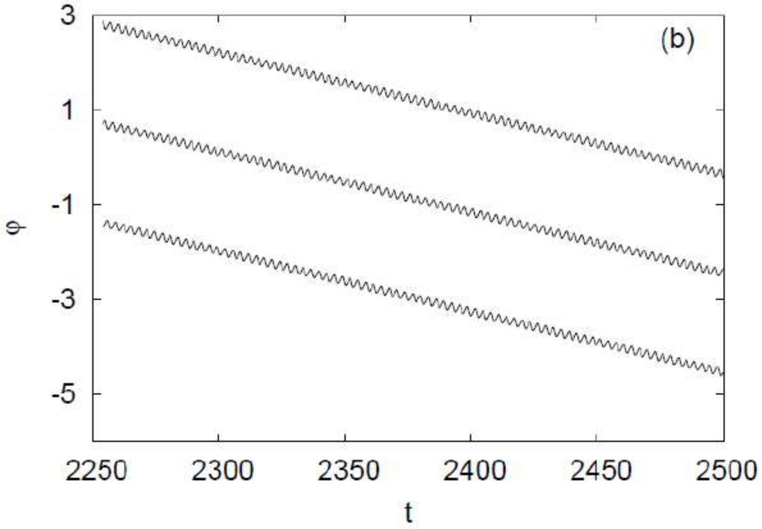

FIG. 2. Particle phase in swarm at initial time interval starting from random initial conditions (a). Synchronized rotations of bacteria in swarm after establishment of the order (b). $N = 3$ and $\lambda = -0.1$.

Fig.20

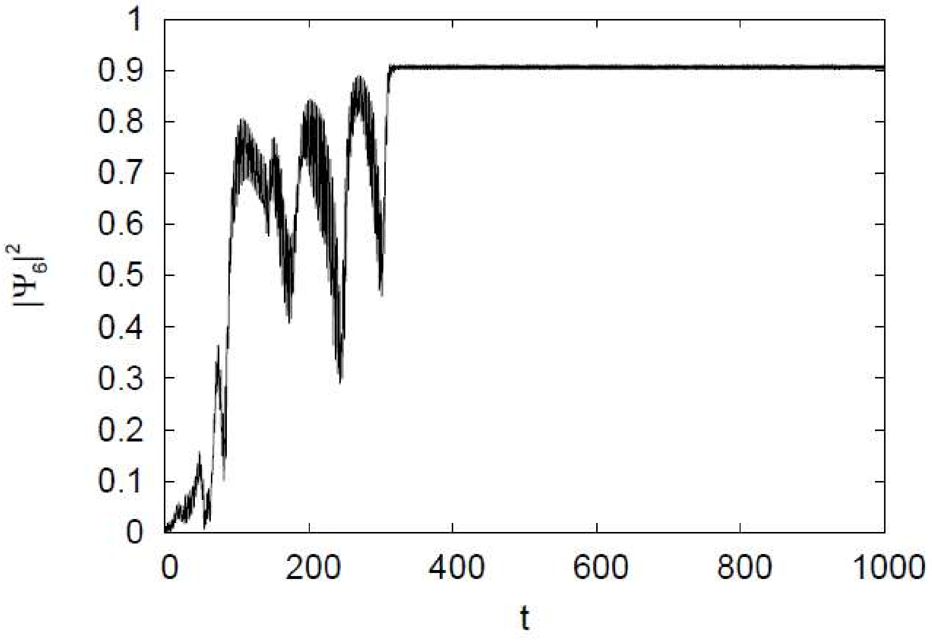

Fig.21

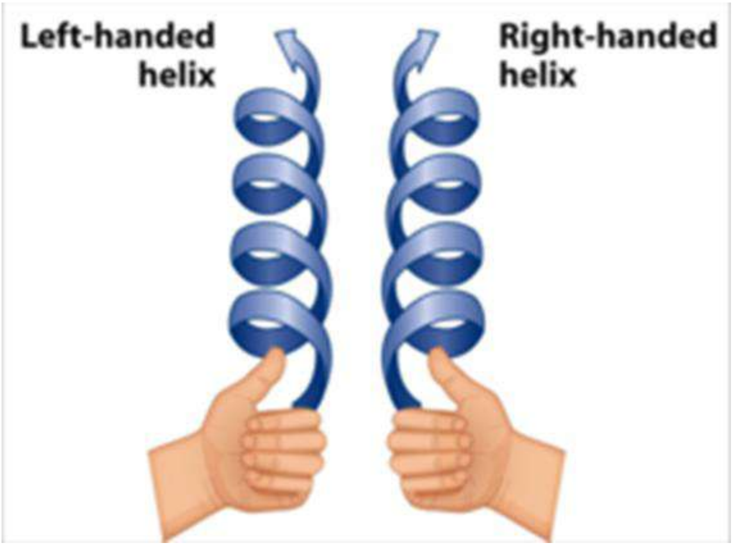

Fig.22